Role of eastward propagating convection systems in the diurnal cycle and seasonal mean of summertime rainfall over the U.S. Great Plains

Xianan Jiang,[1] Ngar-Cheung Lau,[2] and Stephen A. Klein[3]

[1] By diagnosing the 3-hourly North American Regional Reanalysis rainfall data set for the 1979–2003 period, it is illustrated that the eastward propagation of convection systems from the Rockies to the Great Plains plays an essential role for the warm season climate over the central U.S. This eastward propagating mode could be the deciding factor for the observed nocturnal rainfall peak over the Great Plains. The results also suggest that nearly half of the total summer mean rainfall over this region is associated with these propagating convection systems. For instance, the extreme wet condition of the 1993 summer may be attributed to the frequent occurrence of propagating convection events and enhanced diurnal rainfall amplitude over the Great Plains. Thus, proper representation of this important propagating component in GCMs is essential for simulating the diurnal and seasonal mean characteristics of summertime rainfall over the central US. **Citation:** Jiang, X., N.-C. Lau, and S. A. Klein (2006), Role of eastward propagating convection systems in the diurnal cycle and seasonal mean of summertime rainfall over the U.S. Great Plains, *Geophys. Res. Lett.*, *33*, L19809, doi:10.1029/2006GL027022.

1. Introduction

[2] The warm season climate over the continental U.S. is noted for its pronounced diurnal rainfall variability. The precipitation over the U.S. Great Plains (GP) exhibits a nocturnal diurnal peak, in stark contrast to the afternoon rainfall maximum over most inland regions [*Wallace*, 1975; *Riley et al.*, 1987; *Dai et al.*, 1999; *Tian et al.*, 2005]. Figure 1a illustrates the diurnal cycle of rainfall over the GP (100–90°W; 35–45°N), as obtained from North American Regional Reanalysis (NARR) data for the 1979–2003 climatology (blue curve), as well as for the individual summers of 1993 (green) and 1988 (red), which are characterized by severe flood and drought conditions, respectively. A distinct nocturnal rainfall peak at 03LT (U.S. Mountain Time Zone) is discernible in the climatological diurnal cycle. Also evident is the relatively stronger diurnal rainfall amplitude during the wet summer of 1993, with the most excessive rainfall being observed during nighttime. In contrast, the diurnal amplitude of rainfall is

rather weak during the dry summer of 1988. Thus, a better understanding of the diurnal variability would contribute to the improvement of prediction skill for the seasonally averaged rainfall anomaly.

[3] Unfortunately, the capability of the current general circulation models (GCMs) to simulate the observed diurnal variation of rainfall over the GP is rather limited [*Dai et al.*, 1999; *Klein et al.*, 2006] (also M.-I. Lee, An analysis of the warm season diurnal cycle over the continental United States and Northern Mexico in general circulation model, submitted to *Journal of Climate*, 2005) (hereinafter referred to as Lee et al., submitted manuscript, 2005). Most of the GCMs yield a daytime rainfall maximum over this region. Considering that the strongest static instability resulting from the surface sensible heat flux is attained in the afternoon, the observed nocturnal rainfall peak over the GP has been attributed to mechanisms that are not directly related to variations in static instability. The candidates for such mechanisms include large-scale boundary-layer convergence by the mountain-induced circulation [*Wallace*, 1975; *Tian et al.*, 2005], the diurnal/semi-diurnal variation of surface pressure associated with tidal modes [*Dai et al.*, 1999], and moisture transports by the low-level jet [*Pitchford and London*, 1962; *Helfand and Schubert*, 1995; *Higgins et al.*, 1997]. Comparison between observations and the corresponding GCM simulations, however, indicates that most of the GCMs are capable of capturing these large-scale features [*Dai and Trenberth*, 2004; *Jiang et al.*, 2006; Lee et al., submitted manuscript, 2005]. Hence the discrepancy between the observed and simulated diurnal cycle of GP rainfall does not appear to be the consequence of inadequate representation of these large-scale processes in the model atmosphere.

[4] *Riley et al.* [1987] and *Carbone et al.* [2002] proposed that the diurnal cycle of rainfall over the GP may be linked to coherent eastward migrating convection systems from the Rockies to the GP. This relationship is illustrated by the time-longitude diagram (Figure 1b) of the climatological diurnal rainfall evolution based on NARR data. This panel shows that convection originates from the ridge of the Rockies during the afternoon, and then propagates eastward with a phase speed of about 22 m/s between 18LT and 06LT. As the convection advances eastward, the rainfall intensifies and attains a maximum at 03LT over the GP. This eastward propagating signal is poorly simulated by the current GCMs (e.g., Lee et al., submitted manuscript, 2005). Thus, the lack of such migratory signals in the GCMs may be a probable cause for the model deficiencies in reproducing the diurnal cycle of rainfall over the GP. Through analysis of the high-resolution NARR data set, we have made an attempt in the present study to explore the role of the eastward propagating

[1]Atmospheric and Oceanic Sciences Program, Princeton University, Princeton, New Jersey, USA.
[2]Geophysical Fluid Dynamics Laboratory/NOAA, Princeton University, Princeton, New Jersey, USA.
[3]Atmospheric Science Division, Lawrence Livermore National Laboratory, Livermore, California, USA.
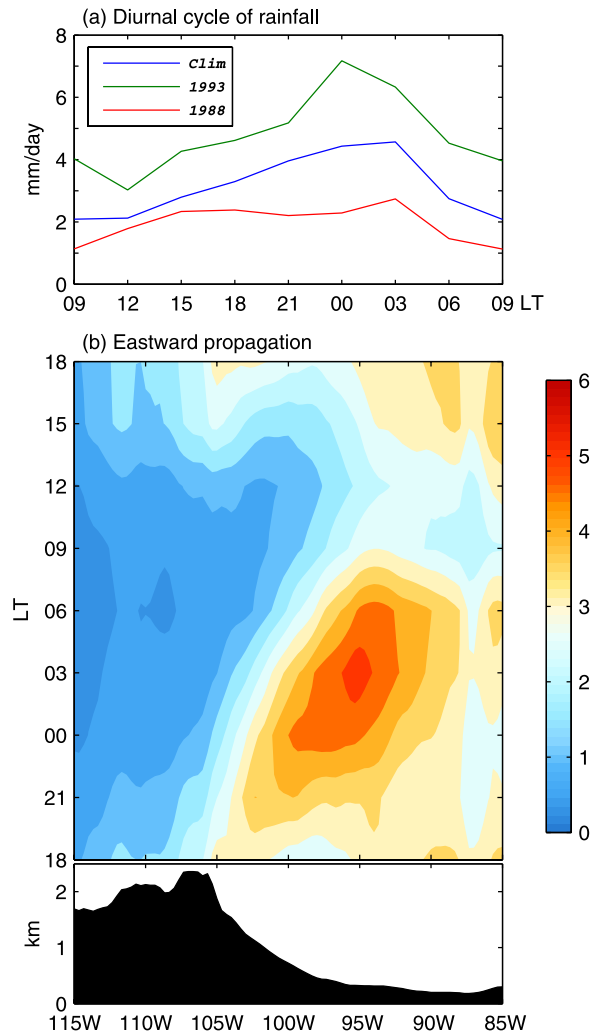
Figure 1. (a) Diurnal cycle of summer (MJJA) rainfall over the Great Plains (100–95°W, 35–45°N), based on climatological average over the 1979–2003 period (blue), and data for the individual summers of 1993 (green) and 1988 (red). (b) Time-longitude distribution of climatological summer mean rainfall (1979–2003) in the 35–45°N zone (units: mm day^{-1}). The longitudinal profile of topography (averaged over 35–45°N) is shown at the bottom.

convective systems in the diurnal cycle and summer mean of rainfall over the GP.

2. Data and Approach

[5] The data set used for this study is the North American Regional Reanalysis [*Mesinger et al.*, 2006]. This data set covers the 25-year period from October 1978 to December 2003, with spatial and temporal resolutions of 32 km and 3 hours, respectively. Data fields are available at 29 vertical levels. The precipitation field in this data set is in very good agreement with rain gauge measurements [*Mesinger et al.*, 2006].

[6] The evolution of rainfall over each 24-hour period is treated as one "diurnal case". There are thus altogether 3025 diurnal cases within the May–August season during the 25-year period covered by the data set. Cases

with very weak diurnal rainfall maxima over the GP (less than 2 mm day^{-1}) are removed from the data set. These excluded cases are mostly clear days over the GP and contribute very little to the total rainfall amount. By doing so, we have a total of 2431 diurnal cases (hereafter *total cases*) available for further analysis. These *total cases* are further categorized into two groups: *nocturnal cases* (1455 cases) with rainfall maximum over the GP occurring during nighttime (21 LT–06 LT), and *non-nocturnal cases* (976 cases) with a rainfall peak during daytime (09 LT–18 LT).

[7] In order to identify the eastward propagating rain episodes and to delineate their contribution to the nocturnal cases, an extended empirical orthogonal function (EEOF [*Weare and Nasstrom*, 1982]) analysis has been conducted on the 3-hourly summer (MJJA) rainfall in the entire 25-year NARR data set for the region (110–90°W; 30–48°N) with 6 temporal lags. Due to computational limitations, rainfall data at every other grid point are employed when conducting the EEOF analysis, i.e., there are 32 by 29 grid points in zonal and meridional directions respectively. The spatial-temporal pattern for the leading mode
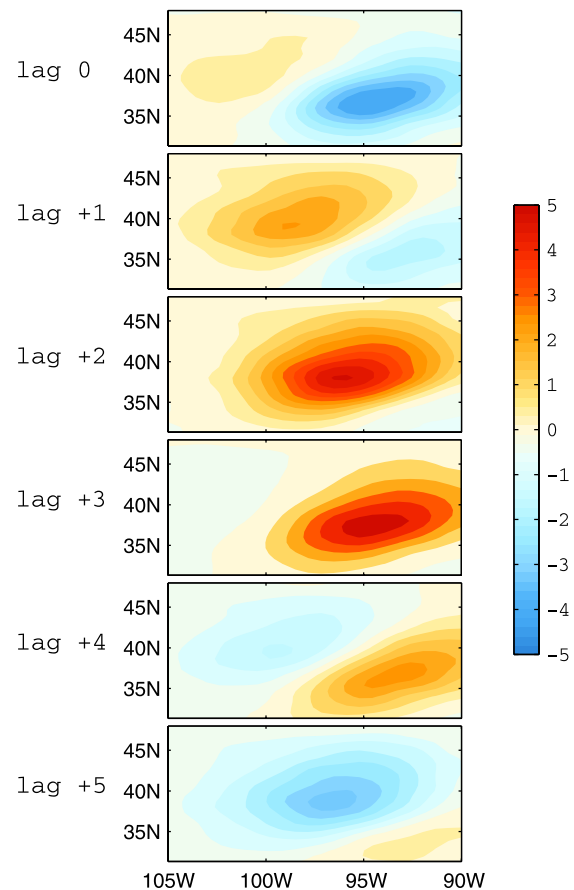

Figure 2. Lagged regression patterns of summertime (May–August) rainfall versus the standardized time series of temporal coefficients for the EEOF1 mode (units: mm day^{-1}). The time interval between adjacent panels is 3 hours. The amplitudes shown here represent the typical rainfall anomalous associated with one standard deviation of the EEOF1 time series.
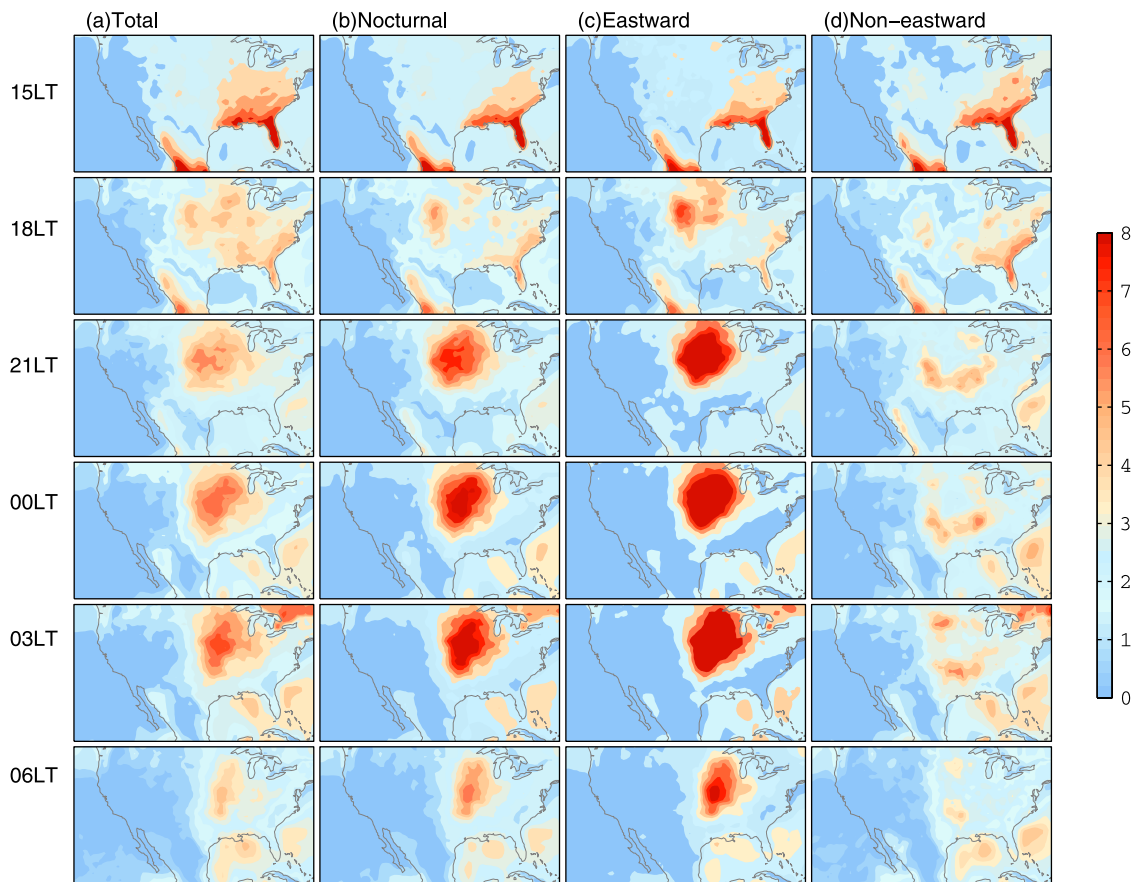
Figure 3. Composite diurnal evolution of rainfall based on the *total cases* (2431 cases), *nocturnal cases* (1455 cases), *eastward cases* (808 cases) and *non-eastward cases* (647 cases). Units: mm day^{-1}. See text for detailed description of the procedures for identifying the four categories of diurnal cases.

(EEOF1), displayed in Figure 2, depicts the essential characteristics of eastward propagating systems over the GP. The EEOF2 mode (figure not shown), is in quadrature with the EEOF1, and exhibits the same propagation behavior as illustrated in Figure 2. This first pair of EEOFs explains 5.2% of the total variance. The time series of temporal coefficients associated with EEOF1 will serve as the basis for detecting the occurrence of the eastward propagating convective episodes.

3. Results

[8] Figure 3a displays the composite diurnal rainfall evolution over the U.S. based on the 2431 *total cases*. In accord with Figure 1b, convection first appears over the ridge of the Rockies at about 15LT. It then intensifies quickly and moves eastward toward the GP. At 03LT, the convection center is located over the GP and attains its maximum amplitude. These features are clearly discernible in the composite over the *nocturnal cases* (Figure 3b). The composite over the *non-nocturnal cases* (figure not shown) displays a rainfall peak over the GP at 18LT with rather weak and poorly organized convection during nighttime over this region, and bears a close resemblance to the typical diurnal cycle of precipitation over land.

[9] Two criteria have been applied to the EEOF1 time series to identify those *nocturnal cases* in which eastward

propagating precipitating systems are prominent: Peak of the time series for each of the selected days must exceed one standard deviation; and the peak must occur between 12LT and 21LT. The second criterion ensures that the eastward propagating system contributes to maximum rainfall over the GP during nighttime (see the space-time evolution of the EEOF1 mode in Figure 2). On the basis of this selection scheme, 808 of the 1455 *nocturnal cases* are classified as episodes with strong eastward propagating signals (hereafter *eastward cases*); whereas the remaining 647 events are not clearly linked to eastward migration (*non-eastward cases*). The composite diurnal rainfall evolutions for the *eastward* and *non-eastward cases* are displayed in Figures 3c and 3d, respectively. It is readily seen that the essential features in the composite over the *nocturnal cases* are very similar to those in the composite for the *eastward cases*. On the contrary, the corresponding pattern for the *non-eastward cases* displays weak and unorganized centers over the GP.

[10] Figure 4 illustrates in a cumulative fashion the diurnal evolution of precipitation over the GP associated with three categories of diurnal cases: *non-nocturnal, non-eastward* and *eastward cases*. It shows the afternoon peak (18LT) over the GP during the *non-nocturnal cases*, as previously mentioned. The rainfall in *non-eastward cases* is relatively weak. The summation over rainfall in the *non-nocturnal* and *non-eastward cases* still exhibits an afternoon peak. In sharp contrast to these cases, the
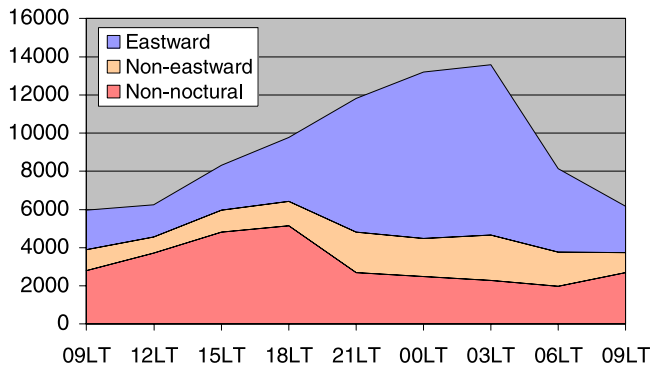
Figure 4. Diurnal evolution of cumulative precipitation over the Great Plains (100−90°W, 35−45°N) due to three categories of diurnal cases: *non-nocturnal*, *non-eastward* and *eastward cases*. Units: mm day^{-1}.

eastward cases are characterized by strong diurnal amplitude with a prominent peak during nighttime. The contribution from these *eastward cases* leads to a cumulative nocturnal rainfall peak as seen earlier in Figure 1a. The relative contributions to total summer rainfall over the GP by the three categories of diurnal cases can be further evaluated by integrating the results in Figure 4 over the entire day. Such calculations reveal that the *non-nocturnal*, *non-eastward* and *eastward cases* account for 34%, 16% and 50% of the total daily mean summer rainfall, respectively. These results suggest that eastward propagating convection systems originating from the Rockies play an essential role for both the diurnal cycle and summer mean rainfall over the GP.

[11] Further analysis indicates that this eastward propagating mode is relatively inactive during early May. The propagating events become progressively more active with the advance of the summer season, with maximum frequency of occurrence during late June and early July. This result is largely consistent with those by *Carbone et al.* [2002] based on radar observations for four years.

[12] Figure 5 illustrates the interannual variation of the number of eastward propagating cases during individual summers of the 1979−2003 period (black curve), as well as the summer mean rainfall over the GP (blue curve). A strong correspondence between the two curves is evident. The correlation between these two time series is 0.76. Especially note-worthy are that the 1993 maxima and 1988 minima in the two curves. As noted in the discussion of Figure 1a, extreme wet and dry conditions prevailed during the summers of 1993 and 1988, with enhanced and reduced diurnal amplitudes, respectively. Hence the result in Figure 5 further demonstrates the important role of the eastward propagating mode in the diurnal cycle of rainfall over the GP.

[13] To document the prevalent large-scale circulation features accompanying the eastward propagating events, a composite analysis over the strong *eastward cases* (with amplitudes in the EEOF1 time series exceeding two standard deviations) has been performed for the daily averaged geopotential height (ϕ), specific humidity (q) and wind fields at various vertical levels. The climatological means have been removed from these composites and the results

are displayed in Figure 6. Figures 6a and 6b show the longitude-pressure distributions of ϕ and q for the 35−45°N zone. During strong eastward propagating cases, negative perturbations of ϕ are seen to prevail through the entire troposphere over the Rockies, with largest amplitudes being located at about 250mb. In the lower troposphere, the ϕ perturbations exhibit an eastward shift with decreasing altitude towards the GP. Positive ϕ perturbations are evident over the eastern U.S. Meanwhile, enhanced specific humidity is found over the GP extending from the surface to 200mb (Figure 6b). The horizontal patterns of geopotential height and wind fields over the 850mb (Figure 6c) suggest an enhanced southerly low-level jet between the negative and positive ϕ centers. This enhanced low-level jet over the GP is coincident with enhanced specific humidity center over this region (Figure 6d). These anomalies are reminiscent of the large-scale pattern during the extreme wet summer of 1993 [*Kunkel et al.*, 1994; *Mo et al.*, 1995; *Ting and Wang*, 2006].

4. Summary and Discussion

[14] Through analysis of the long-term NARR rainfall data set, it is illustrated that the eastward propagating convection systems over the Rockies and the GP play an essential role for the warm season climate over the central U.S. This eastward propagating mode could be the key factor in giving rise to the observed nocturnal rainfall peak over the GP. The results also suggest that nearly half of the total summer mean rainfall over this region could be associated with these propagating convection systems. The important role of this propagating mode is further highlighted by the more frequent occurrence of propagating convection events and more marked diurnal variation of rainfall over the GP during the extreme wet summer of 1993. Note that the statistics examined in this study are based on strong eastward propagating cases with temporal coefficients of the EEOF1 exceeding one standard deviation. This criterion, together with limitations of the NARR data set in representing features with very small spatial and temporal scales, could lead to underestimation of the contribution of this mode to the local rainfall. An indepen-
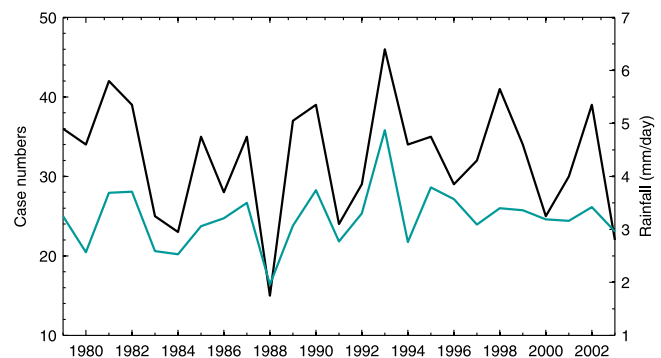

Figure 5. Interannual variations of the frequency of occurrence of eastward propagating cases during summer (black curve, left ordinate); and of summer mean rainfall over the Great Plains (100−90°W, 35−45°N; blue curve, right ordinate). The summer season is defined as the May− August period.
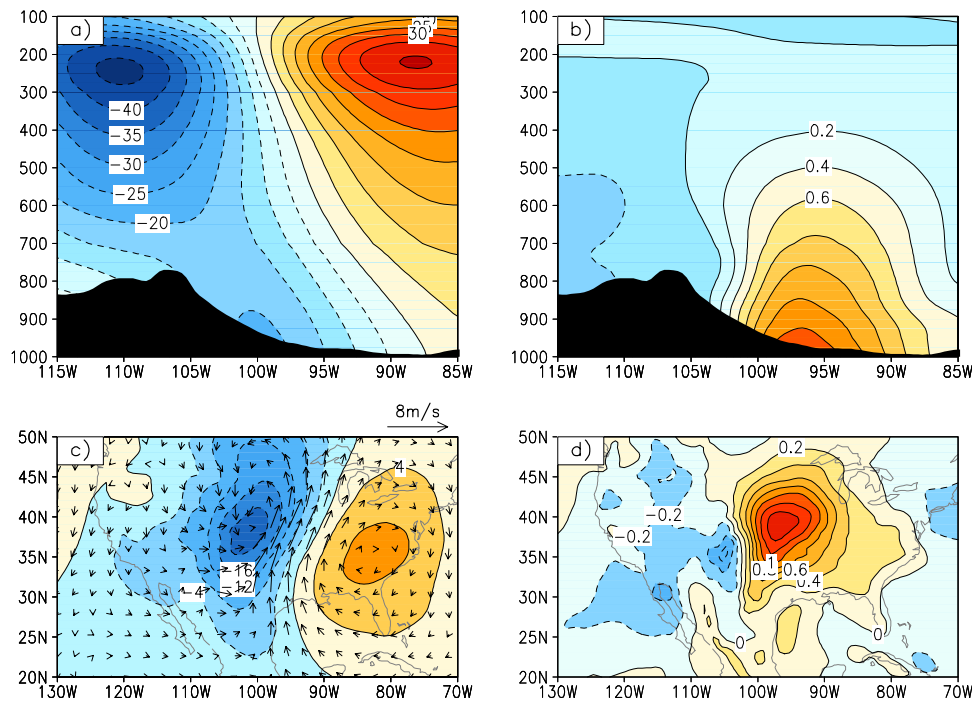
Figure 6. Composites of large-scale perturbation patterns accompanying the strong eastward propagating cases: Longitude-pressure distributions of (a) geopotential height (units: gpm) and (b) specific humidity (units: g/kg), averaged over the 35–45°N zone; (c) horizontal distributions of the geopotential height (contours; units: gpm) and wind vectors, and (d) specific humidity (units: $k \ kg^{-1}$), all at 850mb. The topography is indicated using dark shading in Figures 6a and 6b. All patterns depict departures from the summer mean climatology.

dent study based on radar observations for nine summer seasons suggest that as much as 2/3 of the diurnal rainfall over this region could be attributed to propagating convection systems (R. Carbone and J. Tuttle, personal communication, 2006). Thus, inadequate representation of this important propagating component in the GCMs could account for the model deficiency in simulating the diurnal variation of summertime rainfall over the central U.S.

[15] The reasons for the lack of eastward propagating precipitation systems in GCM atmospheres remain to be determined. This phenomenon may be associated with the gravity waves or gravity currents [*Carbone et al.*, 2002]. Thus, the relatively coarse horizontal resolution of most GCMs could be a contributing factor to the weak amplitudes of this propagating mode in the simulations. Experiments using various GCMs with increased horizontal resolution (~50 km), however, do not show significant improvement in capturing these propagating signals (figure not shown). A study by *Liang et al.* [2004], based on a regional climate model, suggests that simulation of this eastward propagating mode is sensitive to the cumulus parameterization scheme used in the model. With a common horizontal resolution of 30 km, application of the Grell scheme [*Grell*, 1993] in the model yields a realistic simulation of the eastward propagating convection systems, and thus an improved diurnal cycle of rainfall over the GP; whereas model runs with the Kain-Fritsch [*Kain and Fritsch*, 1993] scheme fail to capture the propagating mode. The responsiveness of the Grell scheme to large-scale tropospheric forcing might partially explain its ability to generate the propagating signal; whereas the excessive

influences of boundary layer forcing in the Kain-Fritsch scheme might hinder the simulation of the migratory disturbances. In view of the significant impacts of these propagating systems on the warm season climate over the U.S., further investigation is warranted to understand the aforementioned GCM deficiencies, as well as the physical mechanisms associated with this propagating mode.

References

Carbone, R. E., J. D. Tuttle, D. A. Ahijevych, and S. B. Trier (2002), Inferences of predictability associated with warm season precipitation episodes, *J. Atmos. Sci.*, *59*, 2033–2056.

Dai, A., and K. E. Trenberth (2004), The diurnal cycle and its depiction in the Community Climate System Model, *J. Clim.*, *17*, 930–951.

Dai, A., F. Giorgi, and K. E. Trenberth (1999), Observed and model simulated precipitation diurnal cycle over the contiguous United States, *J. Geophys. Res.*, *104*, 6377–6402.

Grell, G. A. (1993), Prognostic evaluation of assumptions used by cumulus parameterizations, *Mon. Weather Rev.*, *121*, 764–787.

Helfand, H. M., and S. D. Schubert (1995), Climatology of the Great Plains low-level jet and its contribution to the continental moisture budget of the United States, *J. Clim.*, *8*, 784–806.

Higgins, R. W., Y. Yao, E. S. Yarosh, J. E. Janowiak, and K. C. Mo (1997), Influence of the Great Plains low-level jet on the summertime precipitation and moisture transport over the central United States, *J. Clim.*, *10*, 481–507.

Jiang, X., N.-C. Lau, I. M. Held, and J. Ploshay (2006), Mechanisms of the Great-Plains Low-level Jet as simulated in an AGCM, *J. Atmos. Sci.*, in press.

Kain, J. S., and J. M. Fritsch (1993), Convective parameterization in mesoscale models: The Kain-Fritsch scheme, in *The Representation of Cumulus Convection in Numerical Models*, *Meteorol. Monogr.*, *46*, 165–170.

Klein, S. A., X. Jiang, J. Boyle, S. Malyshev, and S. Xie (2006), Diagnosis of the summertime warm and dry bias over the U.S. Southern Great Plains in the GFDL climate model using a weather forecasting approach, *Geophys. Res. Lett.*, *33*, L18805, doi:10.1029/2006GL027567.

Kunkel, K. E., S. A. Changnon, and J. R. Angel (1994), Climate aspects for the 1993 upper Mississippi River basin flood, *Bull. Am. Meteorol. Soc.*, *75*, 811–822.

Liang, X.-Z., L. Li, A. Dai, and K. E. Kunkel (2004), Regional climate model simulation of summer precipitation diurnal cycle over the United States, *Geophys. Res. Lett.*, *31*, L24208, doi:10.1029/2004GL021054.

Mesinger, F., et al. (2006), North American Regional Reanalysis, *Bull. Am. Meteorol. Soc.*, *87*, 343–360.

Mo, K. C., J. Nogues-Paegle, and J. Paegle (1995), Physical mechanisms of the 1993 summer floods, *J. Atmos. Sci.*, *52*, 879–895.

Pitchford, K. L., and J. London (1962), The low-level jet as related to nocturnal thunderstorms over midwest United States, *J. Appl. Meteorol.*, *1*, 43–47.

Riley, G. T., M. G. Landin, and L. F. Bosart (1987), The diurnal variability of precipitation across the central Rockies and adjacent Great Plains, *Mon. Weather Rev.*, *115*, 1161–1172.

Tian, B., I. M. Held, N. Lau, and B. J. Soden (2005), Diurnal cycle of summertime deep convection over North America: A satellite perspective, *J. Geophys. Res.*, *110*, D08108, doi:10.1029/2004JD005275.

Ting, M., and H. Wang (2006), The role of the North American topography on the maintenance of the Great Plains summer low-level jet, *J. Atmos. Sci.*, *63*, 1056–1068.

Wallace, J. M. (1975), Diurnal variations in precipitation and thunderstorm frequency over the conterminous United States, *Mon. Weather. Rev.*, *103*, 406–419.

Weare, B. C., and J. S. Nasstrom (1982), Examples of extended empirical orthogonal function analysis, *Mon. Weather. Rev.*, *110*, 481–485.

———————————

X. Jiang and N.-C. Lau, NOAA/Geophysical Fluid Dynamics Laboratory, Princeton University, Forrestal Campus, P.O. Box 308, Princeton, NJ 08542, USA. (xianan.jiang@noaa.gov)

S. A. Klein, Atmospheric Science Division (L-103), Lawrence Livermore National Laboratory, P.O. Box 808, Livermore, CA 94551, USA.